

BOOSTING FACIAL ACTION UNIT DETECTION THROUGH JOINTLY LEARNING FACIAL LANDMARK DETECTION AND DOMAIN SEPARATION AND RECONSTRUCTION

Ziqiao Shang Li Yu*

School of Electronic and Information Communications, Huazhong University of Science and Technology
Wuhan, China

ABSTRACT

Recently how to introduce large amounts of unlabeled facial images in the wild into supervised Facial Action Unit (AU) detection frameworks has become a challenging problem. In this paper, we propose a new AU detection framework where multi-task learning is introduced to jointly learn AU domain separation and reconstruction and facial landmark detection by sharing the parameters of homostructural facial extraction modules. In addition, we propose a new feature alignment scheme based on contrastive learning by simple projectors and an improved contrastive loss, which adds four additional intermediate supervisors to promote the feature reconstruction process. Experimental results on two benchmarks demonstrate our superiority against the state-of-the-art methods for AU detection in the wild.

Index Terms— Facial action unit detection, AU domain separation and reconstruction, Multi-task learning training strategy, Feature alignment scheme

1. INTRODUCTION

Facial Action Coding System (FACS) [1] has proposed a set of 44 facial action units (AUs) that establish a connection between facial muscle movements and facial expressions, allowing for their simulation. Recently, due to the high labor cost to obtain a large number of high-precision AU labels for images, self-supervised learning has garnered significant attention for AU detection [2, 3, 4]. However, most self-supervised frameworks are still trained in laboratory scene, which have low generalization performance in different scenes. Therefore, AU detection has begun to use a large number of unlabeled AU images in the wild. Comparing images captured in controlled laboratory settings to those taken in natural environments, there are notable disparities in various aspects. These disparities encompass variations in facial expressions, poses, ages, lighting conditions, accessories, occlusions, backgrounds, and the overall quality of the images. Therefore, how to make AU detection have strong generalization in the wild is a challenging task.

The field of AU detection in the wild can benefit greatly from a novel facial task called AU domain feature separation and reconstruction. One solution of this task is to learn features that are invariant across different domains [5, 6]. However, this approach may lead to the loss of AU-related information due to the interdependence between AUs and poses, resulting in domain shift. Another solution involves transforming source-domain images to resemble the style of the target domain [7, 8, 9]. Nonetheless, this approach alone may not adequately address other forms of domain shift caused by factors like pose variations and occlusions.

Due to the similarity in feature extraction for facial tasks, multi-task learning training strategies are commonly applied in AU detection [10, 11, 12]. These methods mainly combine AU detection and facial landmark detection, leveraging the similarities between these tasks to enhance performance in each task. Nevertheless, these methods neither solve the problem of relying on impractical and time-consuming manual labeling or inaccurate pseudo labeling techniques, nor do they use precise facial landmarks to guide the process of facial feature separation. And as we know, combining AU domain separation and reconstruction with facial landmark detection for AU detection has never been done before.

To tackle the above issues, this paper proposes a framework for AU detection in the wild, which not only addresses complex labeling with high labor cost, but also solve the problem of additional domain shifts arising from pose variations and occlusions. The main contributions of our work are summarized as follows: (1) We propose a new multi-task learning training strategy to jointly learn AU domain separation and reconstruction and facial landmark detection for AU detection. To our best knowledge, this is the first work to jointly learn these two facial tasks for AU detection. (2) We propose a new feature alignment scheme based on contrastive learning. The simple projectors are developed for magnifying features to the pixel level and an improved contrastive loss adding four additional intermediate supervisors compared to ADLD [9] is proposed for benefitting the features alignment in the reconstruction process. Extensive experiments demonstrate that our method soundly outperforms most state-of-the-art techniques by using unlabeled AU images in the wild.

Author: d202381109@hust.edu.cn

*Corresponding author: hustlyu@hust.edu.cn

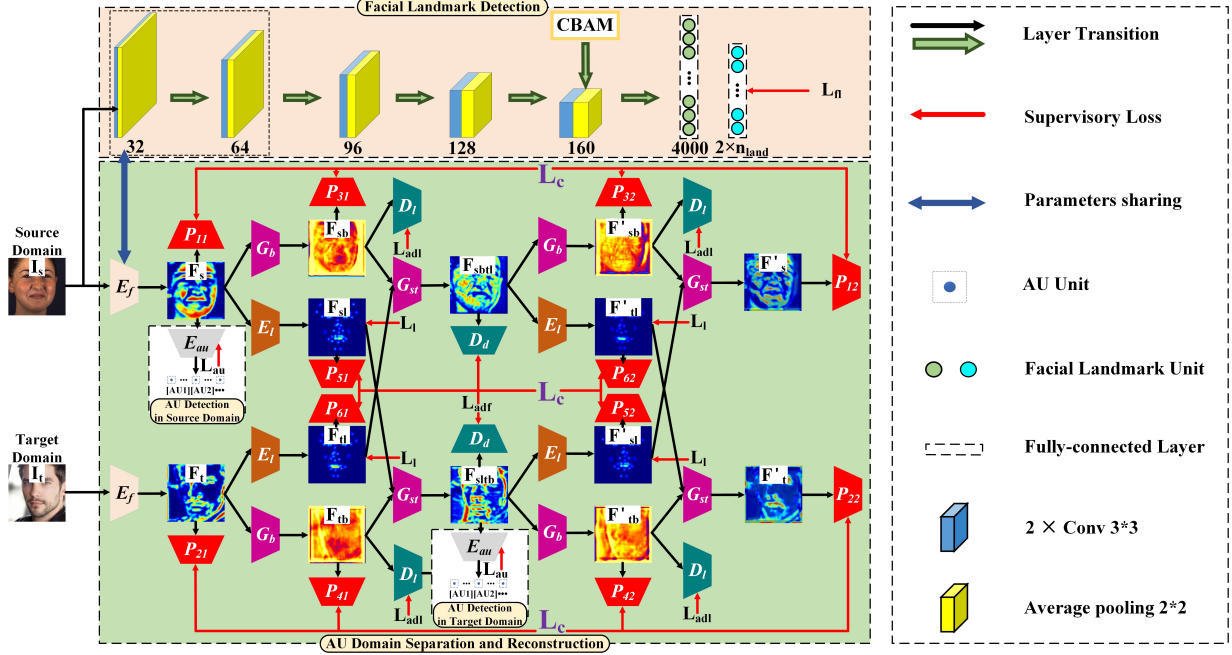


Fig. 1. Overview of our framework, where the same features and modules that have the same structure are marked by the same color. E_f , G_b , E_l , G_{st} , D_l , E_{au} and P_{ij} are shared by source-domain and target-domain input images.

2. OUR PROPOSED METHOD

2.1. Overview

Fig.1 shows the overall architecture of our framework, including two branches: the facial landmark detection branch, and the AU domain separation and reconstruction branch. More details will be introduced in the following.

2.2. Multi-task learning training strategy

As shown in Fig.1, our framework adopts the multi-task learning training strategy, combining the AU domain separation and reconstruction with the facial landmark detection for AU detection. The training strategy consists of two stages. First, we put the source image I_s into the facial landmark detection branch, which contains five parts. Each part comprises two 3×3 convolutional layers with a stride of 1 and padding of 1, and a 2×2 average-pooling layer. After that, the CBAM [13] module is appended. Finally, two fully-connected layers predict facial landmarks trained by L_{fl} as

$$L_{fl}(y, \hat{y}) = -\frac{1}{2d^2} \sum_{i=1}^{n_{land}} [(y_{2i-1} - \hat{y}_{2i-1})^2 + (y_{2i} - \hat{y}_{2i})^2] \quad (1)$$

where y_{2i-1} and y_{2i} represent the actual x-coordinate and y-coordinate of the i -th facial landmark, while \hat{y}_{2i-1} and \hat{y}_{2i} represent the corresponding predicted values. n_{land} denotes the total number of facial landmarks, and d represents the inter-ocular distance of two eyes used for normalization.

After the training of facial landmark detection branch, we put both the source image I_s and the target image I_t into the feature extraction module E_f with initialized parameters provided by the first two parts of the facial landmark detection branch, since E_f has the same structure as the two parts. Then we train both branches simultaneously. The advantage of this approach is that it enables weight sharing of partial modules for the two facial tasks with similar facial features, which can mutually guide each other during training. The initialized parameters also help E_f warm up before training to facilitate the separation process.

2.3. AU Domain Feature Separation and Reconstruction

The whole separation and reconstruction process contains two branches, the source domain branch and the target domain branch. Each branch is separated and reconstructed twice. The source image I_s and the target image I_t are first put into the feature extraction module E_f with initialized parameters to get AU features F_s and F_t . Then, a facial texture encoder E_l and a background feature generator G_b are used to separate F_s and F_t into landmark-related features F_{sl} and F_{tl} , and background features F_{sb} and F_{tb} . A minimax game theory is employed in the process of feature separation where the first generator G_b attempts to generate background features, while the first discriminator D_l aims to detect landmark-related features in the generated background features. After that, another generator G_{st} is applied to generate new reconstructed features F_{sltb} and F_{sttl} by combining F_{sl} and F_{tb} , F_{sb} and

F_{tl} . Another discriminator D_d is used to recognize generated features from other domains. Finally, another round of domain separation and reconstruction which is the same as the first round is introduced to F_{sltb} and F_{sbtlt} to obtain cross-cyclically reconstructed original features F'_s and F'_t . The details of the minimax game theory and the introduced losses including L_l , L_{adf} and L_{adl} can refer to ADLD [9].

2.4. Feature Alignment scheme and AU detection

To better reconstructed features, we propose a new feature alignment scheme based on contrastive learning, which is realized by projectors $P_{ij}(\cdot)$ and an improved contrastive loss L_c . Specifically, the contrastive loss adds four intermediate supervisors between F'_{sl} and F_{sl} , F'_{sb} and F_{sb} , F'_{tl} and F_{tl} , F'_{tb} and F_{tb} in addition to the two reconstructed pairs F'_s and F_s , F'_t and F_t . The contrastive loss L_c is formally the L_1 loss:

$$L_c = \frac{1}{h_s \times w_s} \sum_{h_s, w_s} \|F'_s - F_s\| + \frac{1}{h_t \times w_t} \sum_{h_t, w_t} \|F'_t - F_t\| \\ + \frac{1}{h_{sl} \times w_{sl}} \sum_{h_{sl}, w_{sl}} \|F'_{sl} - F_{sl}\| + \frac{1}{h_{sb} \times w_{sb}} \sum_{h_{sb}, w_{sb}} \|F'_{sb} - F_{sb}\| \\ + \frac{1}{h_{tl} \times w_{tl}} \sum_{h_{tl}, w_{tl}} \|F'_{tl} - F_{tl}\| + \frac{1}{h_{tb} \times w_{tb}} \sum_{h_{tb}, w_{tb}} \|F'_{tb} - F_{tb}\| \quad (2)$$

where h and w denote the spatial locations of each features. The projectors $P_{ij}(\cdot)$ are added after each reconstructed feature to match the feature dimensions by a relatively simple structure while being efficient enough to ensure accurate alignment, where i represents each supervisor pair and j represents the feature number of each supervisor pair. In fact, this simple loss has already been utilized before [14, 15, 16], but we are actually trying to reveal the potential value of the additional intermediate supervisors rather than designing a complicated loss for feature alignment. The advantage of this approach is that it achieves pixel-by-pixel alignment of the face-background features and the intermediate supervisions greatly improve the reconstruction process.

F_s and F_{sltb} are respectively introduced into the AU detector F_{au} , using the weighted multi-label cross entropy loss L_{au} [10, 17, 18] for AU detection. Combining all the losses, we yield the overall objective function:

$$L_{all} = \lambda_c L_c + \lambda_l L_l + \lambda_{adl} L_{adl} + \lambda_{adf} L_{adf} + \lambda_{au} L_{au} + \lambda_{fl} L_{fl} \quad (3)$$

where the hyperparameters $\lambda_{(\cdot)}$ are utilized to control the relative significance of each loss term in our framework.

3. EXPERIMENTS

3.1. Experiment Settings

3.1.1. Datasets

In our experiments, we utilized two widely-used datasets for AU detection: BP4D [19] for the supervised source do-

main and EmotioNet [20] for the unsupervised target domain. BP4D consists of a total of 140,000 frames in laboratory scene with 12 AU labels and 68 facial landmarks. EmotioNet consists of around 1,000,000 unlabeled images sourced from the Internet and 21,088 labeled images. We randomly selected 200,000 unlabeled images as the training set and divided all labeled images into a validation set (10,544 images) and a test set (10,544 images). To tackle the problem of data imbalance, our framework evaluation focuses solely on 6 AUs (AU1, AU2, AU4, AU6, AU12, AU17) with occurrence rates exceeding 7% in both BP4D and EmotioNet. The package dlib was used to annotate all 68 landmarks, and any images without detected landmarks were subsequently excluded from the dataset.

3.1.2. Implementation Details

For both datasets, images are augmented through similarity transformation including in-plane rotation, uniform scaling, and translation by 68 facial landmarks to the same resolution of $3 \times 200 \times 200$ pixels, and randomly cropped into 176×176 pixels with random horizontal flip. We conduct training experiments on one NVIDIA GeForce RTX 2080Ti GPU with 11GB for two days and implement them by using PyTorch. Firstly, we pretrain the facial landmark detection branch with a learning rate of 0.0001, a batchsize of 8 and 20 epochs. The number of facial landmarks n_{land} is 49, which exclude the facial contour landmarks. Secondly, the feature extractor E_f loads pre-training parameters and trains the whole framework for up to 12 epochs. The learning rate is also 0.0001 during the first 4 epochs and linearly decayed every 4 epochs. Thirdly, we choose the pre-trained model with the best performance and fine-tune it. To better set appropriate values for the trade-off parameters λ_c , λ_l , λ_{adf} , λ_{adl} , λ_{au} and λ_{fl} , we use the control variable method to change only one parameter every time and set λ_c , λ_l , λ_{adf} , λ_{adl} , λ_{au} and λ_{fl} to 100, 0.6, 1.2, 400, 1 and 0.1 respectively by verification experiments. This also illustrates that our proposed contrastive loss takes a large proportion, which has great effect on training. The evaluation metrics of AU detection are F1-score and Accuracy.

3.2. Comparison with State-of-the-Art Methods

3.2.1. AU Detection in Target Domain

We compare our AU detection results in target domain to traditional adversarial domain adaptation methods including DANN [5], ADDA [6], which learn domain invariant features, and T²Net [8], DRIT [7], ADLD [9], which transfer the source-style images into target-style images. Quantitative results on the target domain dataset EmotioNet when the source domain is BP4D are summarized in Table 1, where our method achieves the best overall performance.

Compared to domain-invariant features learning approaches, namely DANN and ADDA, our method achieves an

average increase of 17.4% and 16.8%. This occurs because by enforcing domain invariance of features when feeding them into the AU detector F_{au} , essential AU-related information may be overlooked. Compared to style transfer learning methods, namely T²Net and DRIT, our method outperforms 17.1% and 10.7%. This is attributed to the ability of our approach to overcome the limitations caused by substantial domain shifts, such as variations in pose and occlusion distributions, which can negatively impact target-domain AU detection. Furthermore, our method outperforms 2.1% in F1-score to ADLD, which confirms the effectiveness of multi-task learning training strategy and the additional intermediate supervisions for feature alignment.

Table 1. Comparison of our target domain results and state-of-the-art methods on EmotionNet, where the source domain dataset is BP4D.

Method	Source	AU Index						Avg.
		1	2	4	6	12	17	
DANN [5]	JMLR2016	12.8	6.9	18.9	30.7	53.1	6.3	21.5
T ² Net [8]	ECCV2018	10.1	5.6	21.4	31.3	57.1	5.3	21.8
ADDA [6]	CVPR2017	13.8	6.1	21.4	28.5	57.4	5.1	22.1
DRIT [7]	ECCV2018	18.8	9.0	27.8	40.6	67.9	5.0	28.2
ADLD [9]	TAC2022	19.8	25.2	31.0	58.2	78.3	8.6	36.8
Ours	-	20.2	20.9	34.7	66.0	79.1	12.3	38.9

3.2.2. AU Detection in Source Domain

We also compare our AU detection results in source domain to the methods including Fab-Net [2], ADLD [9], TAE [3], CLP [4] in Tabel 2. These methods are all based on self-supervised framework, but supervised learning is used for experimental verification in source domain.

Although our source domain AU detection network structure is relatively simple, our method achieves an average increase of 8.4%, 1.5%, 0.8% to Fab-Net, TAE, CLP. This is because compared with the methods in laboratory scene, using background information of the images in the wild greatly improves the generalization performance of the framework. The reason for the 1.6% improvement over ADLD is that loading pre-training parameters help F_f warm up before training.

Table 2. Comparison of our source domain results and state-of-the-art methods on BP4D, where the target domain dataset is EmotionNet.

Method	Source	AU Index						Avg.
		1	2	4	6	12	17	
Fab-Net [2]	BMVC2018	43.3	35.7	41.6	72.9	83.5	48.2	54.2
ADLD [9]	TAC2022	50.5	35.7	61.8	74.1	75.2	69.0	61.0
TAE [3]	TPAMI2022	47.0	45.9	50.9	74.7	85.6	62.3	61.1
CLP [4]	TIP2023	47.7	50.9	49.5	75.8	84.1	62.7	61.8
Ours	-	52.0	37.9	61.2	77.1	76.0	71.5	62.6

3.3. Ablation Study

Quantitative results of our framework with different component combinations are summarized in Table 3, including the baseline (BL), the multi-task learning training strategy (ML), and the feature alignment scheme based on contrastive learning (AS). The introduction of ML helps achieve an increase of 1.0% in F1-score and 0.7% in Accuracy, validating that weight sharing of partial modules for two similar facial tasks can mutually guide each other during training. Adopting AS for AU domain reconstruction leads to an increase of 1.4% in F1-score and 0.6% in Accuracy compared to model B. It proves that using projectors $P_{ij}(\cdot)$ and the addition of four intermediate supervisors is effective.

Table 3. F1-scores on EmotionNet when the source domain is BP4D for ablation study.

Model	BL	ML	AS	F1-Score	Accuracy
A	✓			36.5	86.4
B	✓	✓		37.5(+1.0)	87.1(+0.7)
C	✓	✓	✓	38.9(+2.4)	87.7(+1.3)

4. CONCLUSION

In this paper, we propose an end-to-end AU detection framework in the wild, consisting of a facial landmark detection branch, and an AU domain separation and reconstruction branch. A multi-task learning training strategy is proposed, which jointly learns AU domain separation and reconstruction and facial landmark detection by sharing the parameters of homostructural facial extraction modules. To enhance the reconstruction process, we propose a feature alignment scheme based on contrastive learning, utilizing simple projectors and an improved contrastive loss, which adds four intermediate supervisions during the reconstruction process. Experimental results demonstrate the superior performance of our framework for AU detection in the wild. More importantly, the strong generalization performance of this framework makes it applicable to various scenarios, such as analyzing human facial behaviors in human-computer interaction, emotion analysis, car-driving monitoring and so on.

Acknowledgement

This work was supported in part by the National Natural Science Foundation of China under Grant 62271220. The computation is completed in the HPC Platform of Huazhong University of Science and Technology.

5. REFERENCES

- [1] Erika L Rosenberg and Paul Ekman, *What the face reveals: Basic and applied studies of spontaneous expression using the Facial Action Coding System (FACS)*, Oxford University Press, 2020.
- [2] Olivia Wiles, A Koepke, and Andrew Zisserman, “Self-supervised learning of a facial attribute embedding from video,” *arXiv preprint arXiv:1808.06882*, 2018.
- [3] Yong Li, Jiabei Zeng, and Shiguang Shan, “Learning representations for facial actions from unlabeled videos,” *IEEE Transactions on Pattern Analysis and Machine Intelligence*, vol. 44, no. 1, pp. 302–317, 2022.
- [4] Yong Li and Shiguang Shan, “Contrastive learning of person-independent representations for facial action unit detection,” *IEEE Transactions on Image Processing*, 2023.
- [5] Yaroslav Ganin, Evgeniya Ustinova, Hana Ajakan, Pascal Germain, Hugo Larochelle, François Laviolette, Mario Marchand, and Victor Lempitsky, “Domain-adversarial training of neural networks,” *The journal of machine learning research*, vol. 17, no. 1, pp. 2096–2030, 2016.
- [6] Eric Tzeng, Judy Hoffman, Kate Saenko, and Trevor Darrell, “Adversarial discriminative domain adaptation,” in *Proc. CVPR*, 2017, pp. 7167–7176.
- [7] Hsin-Ying Lee, Hung-Yu Tseng, Jia-Bin Huang, Maneesh Singh, and Ming-Hsuan Yang, “Diverse image-to-image translation via disentangled representations,” in *Proc. ECCV*, 2018, pp. 35–51.
- [8] Chuanxia Zheng, Tat-Jen Cham, and Jianfei Cai, “T2net: Synthetic-to-realistic translation for solving single-image depth estimation tasks,” in *Proc. ECCV*, 2018, pp. 767–783.
- [9] Zhiwen Shao, Jianfei Cai, Tat-Jen Cham, Xuequan Lu, and Lizhuang Ma, “Unconstrained facial action unit detection via latent feature domain,” *IEEE Transactions on Affective Computing*, vol. 13, no. 2, pp. 1111–1126, 2022.
- [10] Zhiwen Shao, Zhilei Liu, Jianfei Cai, and Lizhuang Ma, “Jaa-net: joint facial action unit detection and face alignment via adaptive attention,” *International Journal of Computer Vision*, vol. 129, pp. 321–340, 2021.
- [11] Shangfei Wang, Yanan Chang, and Can Wang, “Dual learning for joint facial landmark detection and action unit recognition,” *IEEE Transactions on Affective Computing*, 2021.
- [12] Gauthier Tallec, Arnaud Dapogny, and Kevin Bailly, “Multi-order networks for action unit detection,” *IEEE Transactions on Affective Computing*, 2022.
- [13] Sanghyun Woo, Jongchan Park, Joon-Young Lee, and In So Kweon, “Cbam: Convolutional block attention module,” in *Proc. ECCV*, 2018, pp. 3–19.
- [14] Defang Chen, Jian-Ping Mei, Hailin Zhang, Can Wang, Yan Feng, and Chun Chen, “Knowledge distillation with the reused teacher classifier,” in *Proc. CVPR*, 2022, pp. 11933–11942.
- [15] Romero Adriana, Ballas Nicolas, K Samira Ebrahimi, Chassang Antoine, Gatta Carlo, and B Yoshua, “Fitnets: Hints for thin deep nets,” *Proc. ICLR*, vol. 2, pp. 3, 2015.
- [16] Jing Yang, Brais Martinez, Adrian Bulat, and Georgios Tzimiropoulos, “Knowledge distillation via softmax regression representation learning,” in *Proc. ICLR*, 2020.
- [17] Ziqiao Shang, Congju Du, Bingyin Li, Zengqiang Yan, and Li Yu, “Mma-net: Multi-view mixed attention mechanism for facial action unit detection,” *Pattern Recognition Letters*, 2023.
- [18] Jingwei Yan, Boyuan Jiang, Jingjing Wang, Qiang Li, Chunmao Wang, and Shiliang Pu, “Multi-level adaptive region of interest and graph learning for facial action unit recognition,” in *Proc. ICASSP. IEEE*, 2021, pp. 2005–2009.
- [19] Xing Zhang, Lijun Yin, Jeffrey F Cohn, Shaun Canavan, Michael Reale, Andy Horowitz, Peng Liu, and Jeffrey M Girard, “Bp4d-spontaneous: a high-resolution spontaneous 3d dynamic facial expression database,” *Image and Vision Computing*, vol. 32, no. 10, pp. 692–706, 2014.
- [20] C Fabian Benitez-Quiroz, Ramprakash Srinivasan, and Aleix M Martinez, “Emotionet: An accurate, real-time algorithm for the automatic annotation of a million facial expressions in the wild,” in *Proc. CVPR*, 2016, pp. 5562–5570.